Investigation of Area Spectral Efficiency in Indoor Wireless Communications by Blockage Models

Martin Klaus Müller*, Stefan Schwarz*, Markus Rupp

*Christian Doppler Laboratory for Dependable Wireless Connectivity for the Society in Motion
Institute of Telecommunications, Technische Universität Wien
Gusshausstrasse 25/389, A-1040 Vienna, Austria
Email: {mmueller, sschwarz, mrupp}@nt.tuwien.ac.at

***Abstract*—The performance of indoor wireless cellular networks depends on several parameters such as base station density or arrangement, as well as the blockage of the signal by walls. We investigate the dependence of the network performance in terms of coverage probability and also area spectral efficiency in order to demonstrate the influence of the base station density. We analytically derive expressions for both performance metrics including the blockage by walls and compare these results to those of extensive Monte-Carlo simulations. This is performed for different association strategies as well as for random and regular base station placements. It turns out that in general the addition of walls improves the network performance, and does so even more the smaller the base station density becomes.**

***Index Terms*—Blockages, Blockage Modeling, Indoor Communications, Stochastic Geometry, Random Shape Theory, Wireless Communications, Indoor Environments**

I. Introduction

The growth of mobile traffic worldwide is predicted to be dominated by quasi-static indoor users [1], in addition to highly mobile outdoor users [2]. To satisfy the demand of indoor users, more and more buildings will be equipped with dedicated in-building networks, since the supply of wireless connections from the outside is largely impaired by the penetration loss into buildings through windows and walls. While the understanding and modeling of outdoor networks is quite mature, there are still open questions when it comes to understanding the different propagation effects in indoor environments and how they influence the network performance.

Using stochastic geometry to derive coverage and rate of an outdoor wireless network was already described in [3], but without the inclusion of blockages. In [4], random shape theory was employed to characterize the influence on outdoor urban transmission links. The assumptions in [3, 4] were tailored to outdoor scenarios and only impenetrable walls were considered in the performance metrics. While the work of [5] includes the correlation among blockages, only a rather regular building structure is assumed and the derived expressions already become quite involved. As we have shown in [6], the network performance of a real building will be somewhere between a strictly regular structure and a random 2-dimensional wall placement.

The focus of this paper is on modeling the additional wall attenuation in an indoor network by assuming a 2-dimensional random wall placement and integrating this blockage effect in analysis and simulations. We derive expressions for coverage probability and spectral efficiency and subsequently also area spectral efficiency (ASE), dependent on the wall attenuation value and wall density. Scenarios with random and regular base station (BS) placement are compared for various BS densities.

II. System Model

A. Signal Propagation

The focus in this paper is on downlink transmissions in an indoor wireless communication network with multiple base stations. We consider a log-distance dependent path loss described as $l(d) = d^{-\alpha}$. Furthermore, the signal experiences small-scale fading to account for multi-path propagation effects. We assume Rayleigh fading for all links, such that the channel gain between BS and user follows an exponential distribution. We denote the channel gain w.r.t desired BS by $h \sim \exp(\mu)$ and the channel gain for links with interfering BS i by g_i. We additionally assume that h and g_i $\forall i$ to be independent and identically distributed (i.i.d.). Throughout this paper we set $\mu = 1$ for all links.

We model the additional attenuation of the signal added by walls by accumulating the individual penetration loss values of all walls that are blocking the respective signal path. We do not consider reflections from walls in our scenario (as it would, e.g., be done in a ray-tracing tool), but implicitly include multi-path propagation by reflections *inside* of the same room by the small scale fading.

We define our layout to be two-dimensional (and therefore also two-dimensional signal propagation). We presume our network to be interference limited and thus will neglect the influence of noise.

B. Wall Placement Method

To place blockage objects in form of walls in our scenario, we utilize a Boolean scheme. The center points of the walls form a homogeneous Poisson point process (PPP) with density λ'. The length of each wall L_l is randomly chosen from an arbitrary random distribution with mean $\mathbb{E}[L]$. The orientation Θ_l is uniformly distributed in $(0, 2\pi]$. While scenarios created

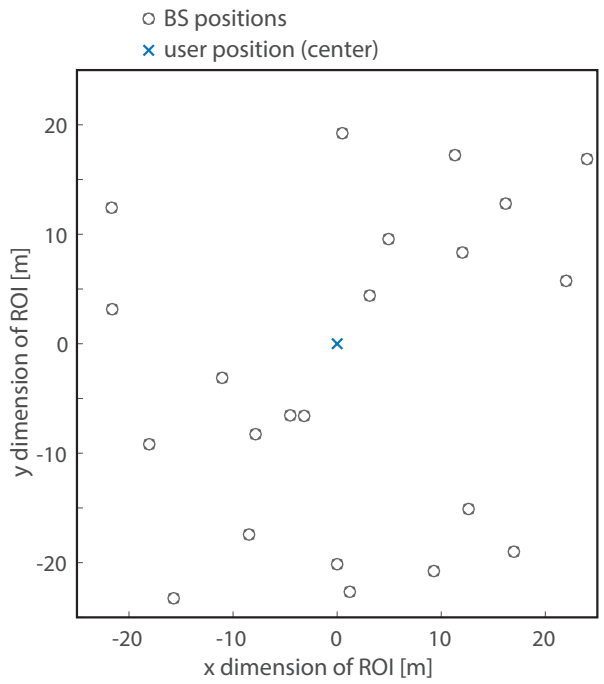

Fig. 1: An example for a realization for random BS placement with BS density λ corresponding to an inter-BS distance $R = 10\,\mathrm{m}$; user always located in center of ROI.

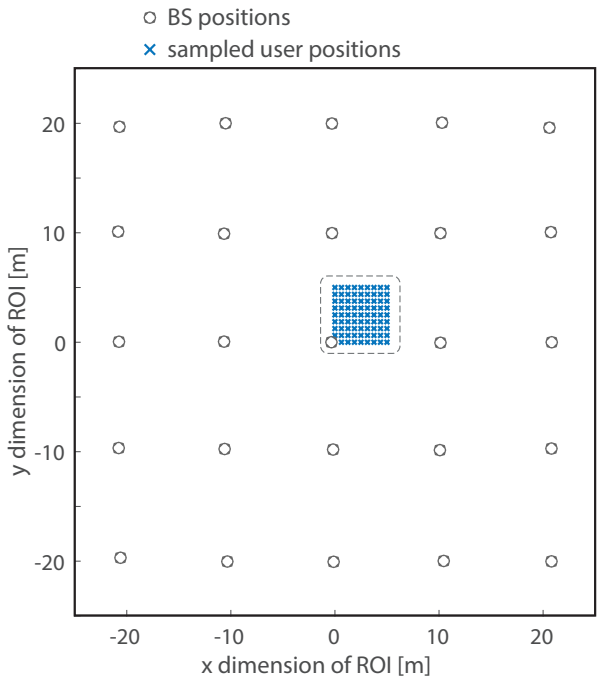

Fig. 2: Regular BS placement for inter-BS distance $R = 10\,\mathrm{m}$ with sampled user positions.

in such a fashion may not appear realistic, they are however easy to treat analytically and represent a worst case w.r.t. signal-to-interference ratio (SIR) performance and blocking of interference (cf. [6]).

The number K of such created walls blocking a link of length d is a Poisson random variable (RV) with mean $\mathbb{E}[K]$, which formulates as (cf. [4]):

$$\mathbb{E}[K] = \beta d = 2/\pi \lambda' \mathbb{E}[L] d, \tag{1}$$

where we subsume the factors that are constant for all links in one scenario into β.

When defining w_l with $0 \leq w_l \leq 1$ as multiplicative factor, representing the wall loss of the l-th wall, then the total attenuation added by walls on a particular link i is $\hat{\omega}_i = \prod_{l=1}^{K_i} w_l$. Throughout this paper we assume the same wall loss for all walls, i.e., $w_l = w$ and thus $\hat{\omega}_i = w^{K_i}$.

C. Transmitter and Receiver Placement

We investigate two kinds of BS placement, namely random and regular placement. The random placement is user-centric and all performance metrics are evaluated for a user in the center of the region of interest (ROI). The BSs are placed according to a homogeneous PPP Φ with density λ. For our analytical performance evaluation, we will consider association of the user to the *closest* BS, while in simulations, we will compare association to the *closest* and the *strongest* BS (cf. Section III).

The inter-BS distance R for the regular BS placement is chosen such that it matches the BS density λ of the BS generating PPP. We consider two full tiers of interferers, which amounts to 25 BSs in total. Due to symmetry, it is sufficient to sample user positions in one quadrant with side-length $R/2$ and evaluate the average performance for all positions. We ensured that the density of samples within the quadrant is large enough to provide statistically accurate results. Since the regular BS placement prohibits closed form analysis we only investigate it by means of simulations.

III. Analytical Description

In this chapter, we derive analytically the performance of an indoor user, in terms of coverage probability and average achievable rate and consequently area spectral efficiency. For these considerations, correlation among blockages on multiple links (i.e., one wall blocking two links at the same time) is ignored. As starting point, we are using the SIR and ignore the influence of noise. For our considered scenarios, it is justified to assume the transmission to be interference limited, as can also be seen in the results of [6].

For all considered propagation effects defined in Section II, the *instantaneous* SIR γ' for a given realization of BSs, walls and fading is described by

$$\gamma' = \frac{P_0 h r^{-\alpha} \hat{\omega}_0}{\sum\limits_{i \in \Phi \setminus b_0} P_i g_i d_i^{-\alpha} \omega_i} = \frac{h r^{-\alpha} w^{K_0}}{\sum\limits_{i \in \Phi \setminus b_0} g_i d_i^{-\alpha} w^{K_i}}, \tag{2}$$

where r denotes the distance of the user from the BS the user is associated with and d_i the distance from interfering BS i.

The transmit power P_i is assumed to be equal for all BSs and therefore cancels out. We denote the desired BS by b_0 and distinguish association to the *closest* BS, which we denote by $b_0^{(c)}$, and association to the *strongest* BS, denoted by $b_0^{(s)}$ accordingly. In a scenario without walls, $b_0^{(c)}$ also corresponds to the strongest BS in the long term average, thus eliminating the influence of the small scale fading.

In (2), the fading, the distance from the user, as well as the number of walls (which in turn is dependent on the distance) are RVs. In order to be able to obtain analytical results, we do not use the actual number of walls K_i, but replace it with its average for a given distance $\mathbb{E}[K_i]$. This is equivalent to assuming a continuous distribution of the wall attenuation along the propagation path, that then only depends on the distance and not on the discrete walls in the scenario. Thus, we eliminate the combinations of discrete wall attenuation values on all BS-user links and simplify the analysis considerably. Consequently, $b_0^{(c)}$ corresponds again to the strongest BS without fading. In the rest of the paper we therefore always assume association to $b_0^{(c)}$ when using a continuous distribution of walls and association to $b_0^{(s)}$ when the discrete realization of walls is considered.

Substituting the instantaneous number of walls K_i with the average $\mathbb{E}[K_i]$ leads to

$$\gamma = \frac{S}{I_r} = \frac{hr^{-\alpha}w^{\mathbb{E}[K_0]}}{\sum\limits_{i\in\Phi\setminus b_0} g_i d_i^{-\alpha} w^{\mathbb{E}[K_i]}} = \frac{hr^{-\alpha}w^{\beta r}}{\sum\limits_{i\in\Phi\setminus b_0} g_i d_i^{-\alpha} w^{\beta d_i}} \tag{3}$$

with β as already defined in (1).

A. Coverage Probability

In the following, we will derive expressions for the coverage probability with the underlying assumptions. The derivation is similar to [3], but with the addition of blockages.

The coverage probability is generally defined as

$$p_c(\delta,\lambda,\alpha) \triangleq \mathbb{P}[\gamma > \delta] \tag{4}$$

where δ is the SIR threshold, above which the user is assumed to be in coverage. Since we defined the distance between the user to its closest/associated BS by r, this also means that the distance d_i of all interfering BSs is *larger* than r and thus there is no BS located in a circle around the user with radius r. Thus, we condition on the distance of the closest BS and average over all possible values of r and additionally apply the void probability probability density function (pdf) $f_r(r) = 2\pi\lambda r e^{-\lambda\pi r^2}$ for no BS being located closer than r. This results in

$$\begin{aligned} p_c(\delta,\lambda,\alpha) &= \mathbb{E}_r\left[\mathbb{P}\left[\gamma > \delta | r\right]\right] \\ &= \int_{r>0} \mathbb{P}[\gamma > \delta |\, r] f_r(r) dr \\ &= \int_{r>0} \mathbb{P}[\gamma > \delta |\, r] e^{-\pi\lambda r^2} 2\pi\lambda r dr. \end{aligned} \tag{5}$$

Plugging in (3) leads to

$$\begin{aligned} p_c(\delta,\lambda,\alpha) &= \int_{r>0} \mathbb{P}\left[\frac{hr^{-\alpha}w^{\beta r}}{I_r} > \delta \middle| r\right] e^{-\pi\lambda r^2} 2\pi\lambda r dr \\ &= \int_{r>0} \mathbb{P}\left[h > \delta r^{\alpha} w^{-\beta r} I_r \middle| r\right] e^{-\pi\lambda r^2} 2\pi\lambda r dr, \end{aligned} \tag{6}$$

where I_r is the resulting accumulated interference for a single spatial realization of BSs.

Next we utilize that h follows an exponential distribution. It follows

$$\begin{aligned} \mathbb{P}\left[h > \delta r^{\alpha} w^{-\beta r} I_r \middle| r\right] &= \mathbb{E}_{I_r}\left[\exp(-\delta r^{\alpha} w^{-\beta r} I_r) \middle| r\right] \\ &= \mathcal{L}_{I_r}(\delta r^{\alpha} w^{-\beta r}) \end{aligned} \tag{7}$$

where $\mathcal{L}_{I_r}(s)$ is the Laplace transform of the RV I_r. Plugging this back in (6) yields

$$p_c(\delta,\lambda,\alpha) = \int_{r>0} \mathcal{L}_{I_r}(\delta r^{\alpha} w^{-\beta r}) e^{-\pi\lambda r^2} 2\pi\lambda r dr \tag{8}$$

with

$$\begin{aligned} \mathcal{L}_{I_r}(\delta r^{\alpha} w^{-\beta r}) &= \mathbb{E}_{\Phi,g_i}\left[\exp\left(-\delta r^{\alpha} w^{-\beta r} \sum_{i\in\Phi\setminus b_0} g_i d_i^{-\alpha} w^{\beta d_i}\right)\right] \\ &\overset{(a)}{=} \mathbb{E}_{\Phi}\left[\prod_{i\in\Phi\setminus b_0} \mathbb{E}_g[\exp(-\delta r^{\alpha} w^{-\beta r} g d_i^{-\alpha} w^{\beta d_i})]\right] \\ &\overset{(b)}{=} \mathbb{E}_{\Phi}\left[\prod_{i\in\Phi\setminus b_0} \frac{1}{1+(r/d_i)^{\alpha} w^{\beta(d_i-r)}\delta}\right] \\ &\overset{(c)}{=} \exp\left(-2\pi\lambda \int_r^{\infty} \left(1 - \frac{1}{1+\left(\frac{r}{v}\right)^{\alpha} w^{\beta(v-r)}\delta}\right) v dv\right) \end{aligned} \tag{9}$$

where (a) follows from all g_i being i.i.d., (b) follows from the exponential distribution of g_i and the last step (c) from the probability generating functional (PGFL) of the PPP [7]. The integral over v corresponds to averaging over the interferer locations for a given r.

B. Area Spectral Efficiency

First we will derive an expression for the spectral efficiency. We assume therefore, that the considered user can reach the (noiseless) Shannon bound $\log_2(1+\gamma)$ by using an adaptive modulation and coding scheme (MCS) and treating interference as noise. For our considered scenario, the spectral efficiency is given by (cf. [3, Appendix C])

$$\begin{aligned} &\tau(\lambda,\alpha) = \mathbb{E}[\log_2(1+\gamma)] \\ &= \int_{r>0} e^{-\pi\lambda r^2} 2\pi\lambda r \int_{t>0} \mathbb{P}\left[\log_2\left(1 + \frac{hr^{-\alpha}w^{\beta r}}{I_r}\right) > t\right] dt\, dr \\ &= \int_{r>0} e^{-\pi\lambda r^2} 2\pi\lambda r \int_{t>0} \mathbb{P}\left[h > (2^t-1) r^{\alpha} w^{-\beta r} I_r\right] dt\, dr \\ &= \int_{r>0} e^{-\pi\lambda r^2} 2\pi\lambda r \int_{t>0} \mathcal{L}_{I_r}(r^{\alpha} w^{\beta r}(2^t-1)) dt\, dr, \end{aligned} \tag{10}$$

with

$$\mathcal{L}_{I_r}(r^\alpha w^{\beta r}(2^t-1)) = \\ = \exp\left(-2\pi\lambda \int_r^\infty \left(1 - \frac{1}{1+\left(\frac{r}{v}\right)^\alpha w^{\beta(v-r)}(2^t-1)}\right) v dv\right), \tag{11}$$

where we performed the same steps as in (6)–(9).

Next we introduce the ASE denoted by κ. This metric better reflects the average cell capacity than the user-centric metrics introduced up to this point. By normalizing the spectral efficiency by the average cell area (which is simply $1/\lambda$), we arrive at the average throughput per Hz per unit area. Thus, it can be described by

$$\kappa(\lambda, \alpha) = \frac{\tau(\lambda, \alpha)}{\mathbb{E}[A^{(cell)}]} = \lambda\tau(\lambda, \alpha). \tag{12}$$

The ASE is an indicator for the average cell capacity that the given network can support. Especially from an operator point of view this is interesting, since it is important to know, e.g., how the cell capacity increases when the total number of installed BSs is increased for a given building/floor.

How the ASE and the aforementioned performance metrics depend quantitatively on the scenario parameters and how the simplifying assumptions for our analytical approach compare against simulation results is discussed in detail in the following section.

IV. Numerical Evaluation

In this section, we present results for the coverage probability p_c and the ASE τ. We compare the (numerically evaluated) resulting values from (8) and (12) with the results of Monte-Carlo simulations. One simulation run for a parameter set is equivalent to one spatial realization of BS locations, one placement of walls including their random orientation and fading realizations. We assume random BS placement for the analytical results, while we simulate both, random and regular BS placement (cf. Figures 1 and 2). For the given wall density λ' and the average wall length $\mathbb{E}[L]$, the average room size is $16\,\mathrm{m}^2$ [1]. We consider the case with no walls ($0\,\mathrm{dB}$ penetration loss) and $3\,\mathrm{dB}$, $6\,\mathrm{dB}$ and $10\,\mathrm{dB}$. (In [8], inner walls are assumed to have $5\,\mathrm{dB}$ penetration loss - thus we cover values with similar magnitude.) The applied parameters are summarized in Table I.

A. Coverage Probability

In this subsection, we only present results for random BS placement. The coverage probability for all three considered values of λ are shown in Figure 3. For each BS density, we show results for all four values of wall attenuation. The results from numerically evaluating (8) are represented by circular markers. Solid lines represent the coverage probability resulting from simulations, based on (3). Additionally, we show results from simulations based on (2) as dashed lines.

[1] this assumes the same average total length of walls per realization, but regular, square rooms of equal size.

TABLE I: Parameters for numerical evaluation

Parameter	Value
path loss exponent	$\alpha = 4$
wall density	$\lambda' = 0.05\,\mathrm{m}^2$
average wall length	$\mathbb{E}[L] = 10\,\mathrm{m}$
wall attenuation	$w_{dB} = \{0, 3, 6, 10\}\,\mathrm{dB}$
inter BS distance	$R = \{10, 30, 60\}\,\mathrm{m}$
resulting BS density	$\lambda \approx \{10^{-2}, 10^{-3}, 3\cdot 10^{-4}\}\,\mathrm{m}^2$
# of BSs (for regular)	25 BSs $\Rightarrow$ 2 rings
spatial realizations	10^5

Several conclusions can be drawn from these results. Firstly, while p_c in (8) still depends on λ, this dependency vanishes for $w = 1$ and $\alpha = 4$ (cf. [3]) and thus, the values are constant for varying densities. The coverage probability improves however for larger wall attenuation values. The improvement is larger for smaller values of λ, since the attenuation is (exponentially) distance dependent and thus by moving the interferers further away, blockages provide a better protection.

Regarding the comparison of analytical results from evaluating (8) and simulations assuming a continuous wall distribution, we see an almost perfect agreement. Small deviations are visible for larger values of λ - these are mostly due to the lack of further interferers by simulating a finite ROI.

Finally, comparing association to $b_0^{(c)}$ and continuous wall distribution with association to $b_0^{(s)}$ and discrete wall realizations, we find that the first setup is only strictly worse for the scenario without blockages (the difference here only stems from the small scale fading). For $w > 1$, this is only true for small values of δ. For larger SIR thresholds, this is no longer the case. Assuming a continuous distribution of walls leads to a guaranteed attenuation of the interference, while in case of discrete walls a dominant interferer can result from a very low number of walls (even as small as for the associated BS) for an unfavorable wall realization.

B. Area spectral efficiency

Next we present results for the ASE. In Figure 4, ASE-results for the same acquisition of performance values as in the previous subsection are presented, namely analytical evaluation of (12) (represented by circular markers), simulation results with association to $b_0^{(c)}$ and continuous wall distribution (represented by solid lines) and simulation results with association to $b_0^{(s)}$ and discrete wall realizations (represented by dashed lines).

Once again the analytical results and the corresponding results from simulations coincide almost perfectly with a small gap due to the finite simulation area. The simulation results for association to $b_0^{(s)}$ are also almost identical, which also fits to the similar behavior of the coverage probability results.

For the comparison of regular and random BS placement, we show simulation results with association to $b_0^{(s)}$ and discrete

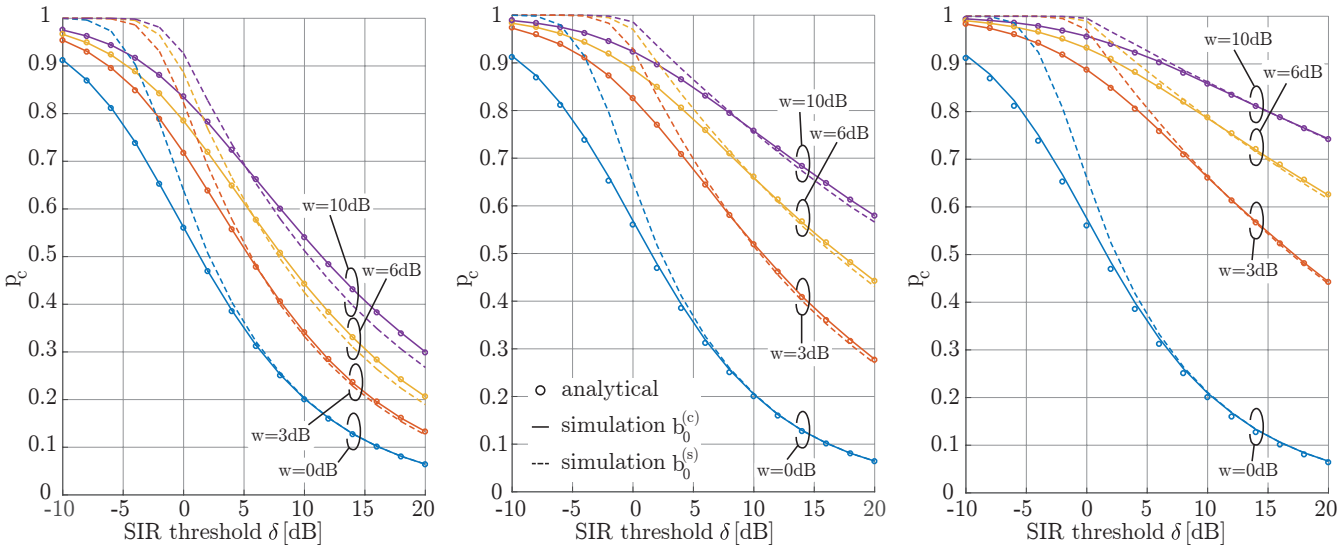

(a) $\lambda = 0.01$. (b) $\lambda = 0.001$. (c) $\lambda = 0.0003$.

Fig. 3: Coverage probability p_c for various BS densities - association to $b_0^{(c)}$: solid lines represent simulation results, circular markers result from evaluating (8); association to $b_0^{(s)}$ represented by dashed lines (simulation results only).

wall realizations. They are presented in Figure 5. Only three penetration loss values are considered, in order to keep the figure readable. Per penetration loss value, results for four configurations are displayed, namely the combinations of random and regular BS placement with association to $b_0^{(c)}$ with continuous wall distribution and association to $b_0^{(s)}$ with discrete wall distribution.

As the results show, the regular BS placement yields a strictly better ASE performance than the random BS placement for all values of w. The slope also remains the same, only a shift is introduced by the regular BS placement.

C. Discussion of Results

Regarding the presented results, there are some interesting conclusions to draw. The influence of the wall parameters (w, λ' and $\mathbb{E}[L]$) is given by their combination $w^{2/\pi\lambda'\mathbb{E}[L]} = w^{\beta}$. As long as this combined factor is not changed, the results stay the same (at least when considering a continuous wall distribution). For all considered scenarios, the addition of walls improves the coverage probability as well as the ASE. This improvement is better for larger sector sizes, since the added attenuation grows faster for the interferers at a larger distance. As it was already shown in [3] for the wall-less scenario, a regular BS placement yields better performance results as a random placement. This remains true for a scenario with walls. Even though we made the simplifying assumption for the analytical derivation to connect to the closest BS and a continuous wall distribution, the averaged performance results in terms of ASE show almost no difference when compared to simulation results where association to $b_0^{(s)}$ and discrete wall realizations is considered.

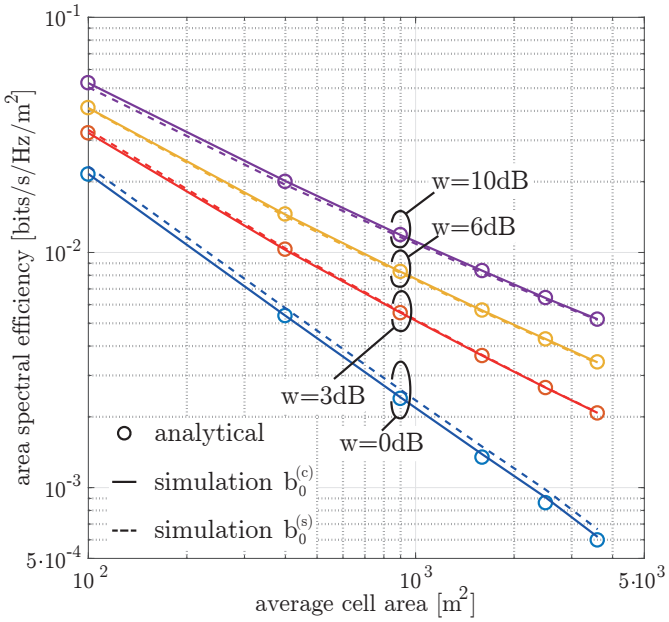

Fig. 4: ASE for different wall attenuations - association to $b_0^{(c)}$: solid lines represent simulation results, circular markers result from evaluating (12); association to $b_0^{(s)}$ represented by dashed lines.

V. Conclusions

In this paper we discussed the influence of randomly distributed wall blockages on the downlink of an indoor cellular network. For random BS placement, we analytically derived expressions for the coverage probability as well as for the ASE. The latter was chosen as performance metric

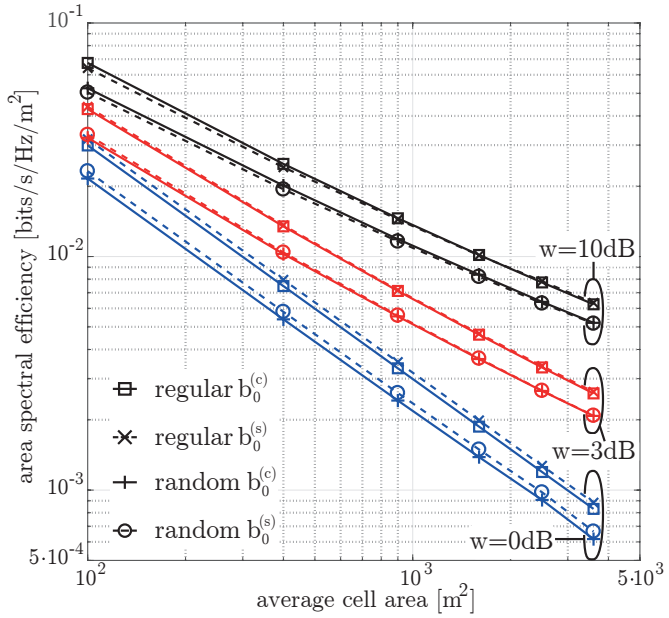

Fig. 5: Comparison of ASE for regular and random BS placement and for different wall attenuations - association to $b_0^{(c)}$ represented by solid lines, to $b_0^{(s)}$ by dashed lines.

in order to demonstrate the influence of the average sector size. Even though some simplifying assumptions were made for our derivations, the resulting performance from the analysis overlaps almost perfectly with results from Monte-Carlo simulations. For all considered parameter combinations, the regular BS placement (only tractable by simulations) always yields an upper bound on the performance of a network with random BS placement.

For future work, an investigation of an even larger parameter-set is planned. Especially results for even larger BS densities might be insightful. Also including the third dimension and a more sophisticated model for the accumulated wall penetration (along the lines of [9]) would make the scenario more realistic. It would also be interesting to consider impenetrable walls, which might be more realistic for upcoming mmWave networks. This would then lead to a distinction of line of sight (LOS) and non line of sight (NLOS) condition of desired and interfering links (see, e.g., [10]). Moreover, the inclusion of the actual wall distribution in our analysis would yield further interesting insights. A promising approach for acquiring the *meta-distribution* of resulting SIR for discrete placement of walls is given in [11]. The network performance for rectangular wall placement (as described in [12]) will also be investigated in the future.

Acknowledgements

This work has been funded by A1 Telekom Austria AG, and the KATHREIN-Werke KG. The financial support by the Austrian Federal Ministry of Science, Research and Economy and the National Foundation for Research, Technology and Development is gratefully acknowledged.

References

[1] Cisco, "Cisco visual networking index: Global mobile data traffic forecast update, 20152020 white paper," Sep. 2016.

[2] S. Schwarz and M. Rupp, "Society in motion: Challenges for LTE and beyond mobile communications," *IEEE Communications Magazine, Feature Topic: LTE Evolution*, vol. 54, no. 5, pp. 76–83, 2016.

[3] J. Andrews, F. Baccelli, and R. Ganti, "A tractable approach to coverage and rate in cellular networks," *IEEE Trans. Commun.*, vol. 59, no. 11, pp. 3122–3134, Nov. 2011.

[4] T. Bai, R. Vaze, and R. W. Heath, "Analysis of blockage effects on urban cellular networks," *IEEE Trans. Wireless Commun.*, vol. 13, no. 9, pp. 5070–5083, Sep. 2014.

[5] J. Lee, X. Zhang, and F. Baccelli, "A 3-D spatial model for in-building wireless networks with correlated shadowing," *IEEE Transactions on Wireless Communications*, vol. 15, no. 11, pp. 7778–7793, Nov. 2016.

[6] M. K. Müller, M. Taranetz, and M. Rupp, "Analyzing wireless indoor communications by blockage models," *IEEE Access*, vol. 5, pp. 2172–2186, 2017.

[7] S. N. Chiu, D. Stoyan, W. S. Kendall, and J. Mecke, *Stochastic Geometry and Its Applications, 3rd Edition*. John Wiley and Sons, Sep. 2013.

[8] 3rd Generation Partnership Project (3GPP), "Evolved Universal Terrestrial Radio Access (E-UTRA); Further advancements for E-UTRA physical layer aspects," 3rd Generation Partnership Project (3GPP), TR 36.814, Mar. 2010.

[9] X. Zhang and J. G. Andrews, "Downlink cellular network analysis with multi-slope path loss models," *IEEE Transactions on Communications*, vol. 63, no. 5, pp. 1881–1894, May 2015.

[10] M. D. Renzo, "Stochastic geometry modeling and analysis of multi-tier millimeter wave cellular networks," *IEEE Transactions on Wireless Communications*, vol. 14, no. 9, pp. 5038–5057, Sep. 2015.

[11] M. Haenggi, "The Meta Distribution of the SIR in Poisson Bipolar and Cellular Networks," *IEEE Transactions on Wireless Communications*, vol. 15, no. 4, pp. 2577–2589, April 2016.

[12] M. K. Müller, M. Taranetz, and M. Rupp, "Effects of wall-angle distributions in indoor wireless communications," in *Int. Workshop Signal Process. Advances in Wireless Commun. (SPAWC'16)*, Jul. 2016, pp. 1–5.